THE ASTROPHYSICAL JOURNAL, 204: 668–683, 1976 March 15

VELOCITY DISPERSIONS AND MASS-TO-LIGHT RATIOS FOR ELLIPTICAL GALAXIES*

S. M. FABER AND ROBERT E. JACKSON
Lick Observatory and Board of Studies in Astronomy and Astrophysics, University of California, Santa Cruz
Received 1975 June 30; revised 1975 August 28

ABSTRACT

Velocity dispersions for 25 galaxies have been measured using conventional and Fourier techniques. The resultant velocity system is probably accurate to 10–15 percent. Internal rms errors are on the order of 10 percent. Using unpublished data of King, we have computed core values of M/L_B. For luminous ellipticals with $M_B < -20$, M/L_B averages $7(H/50\ \mathrm{km\ s^{-1}\ Mpc^{-1}})$, considerably smaller than previous estimates. This value agrees well with M/L_B for early-type spirals, indicating that there is no large discontinuity in M/L_B between ellipticals and early-type spirals. This result is consistent with the observed small color differences between ellipticals and Sa's.

Velocity dispersions increase with luminosity for normal elliptical galaxies of moderate ellipticity. The data also suggest that M/L_B generally increases with luminosity. This conclusion is consistent with predictions based on King's data on core radii and central surface brightness (to be discussed fully in a separate paper). This increase in M/L_B might be due at least in part to the known increase in metal abundance with luminosity for normal elliptical galaxies.

The close correlation between luminosity and dynamical properties for normal ellipticals is further evidence that the ellipticals are very nearly a one-parameter family with total mass as the most important independent variable.

Subject headings: galaxies: internal motions — galaxies: stellar content

I. INTRODUCTION

The measurement of velocity dispersions in early-type galaxies is important for two reasons. Since a considerable fraction of the kinetic energy in these systems is in random motions, a velocity dispersion can be used to estimate the galaxy mass by applying the virial theorem or a related method. Furthermore, because the velocity dispersion has not changed since the initial collapse of the galaxy, it is a clue to processes which occurred during galaxy formation. As pointed out by Fish (1964), the stellar kinetic energy is a measure of the binding energy per particle and hence of the rate at which dissipative processes occur during collapse. For this reason, the velocity dispersion is a critical parameter which must be accounted for by any successful theory of galaxy formation.

Despite the importance of velocity dispersions, relatively few reliable values exist. The largest body of data was collected by Minkowski (1962, and unpublished) using photographic spectra. Recent results (Richstone and Sargent 1972; Morton and Thuan 1973), however, suggest that Minkowski's values may be systematically high.

The data used in the present project were obtained for another purpose: to study variations in line strengths among elliptical and S0 galaxies. However, in the course of reducing the data, it became apparent that the scans also contain considerable information on line-broadening. Hence it seemed desirable to determine velocity dispersions even though the spectral resolution is not quite optimum. The lower limit to the dispersion which can be determined from the present data varies between 100 and 150 km s^{-1}, depending on the signal-to-noise ratio in the scan.

II. OBSERVATIONS AND INITIAL REDUCTION OF DATA

The observational data consisted of scans of the nuclear regions of E and S0 galaxies obtained with the image-dissector scanner (IDS) (Robinson and Wampler 1972) at the Cassegrain focus of the 120 inch (3 m) telescope. The IDS was attached to a conventional Cassegrain spectrograph. A 600 line mm^{-1} grating blazed at 5000 Å was used in first order, which produced a dispersion on the first cathode of the IDS intensifier chain of approximately 110 Å mm^{-1}. At this dispersion, the full width at half-maximum of a neon comparison line is 7 Å in the middle two-thirds of a scan. A slit size of 2″ × 4″ was used for nearly all observations of both stars and galaxies.

The 2048-channel scans cover a wavelength range of roughly 4100 to 6300 Å for all objects. The raw instrumental response of the IDS varies considerably from point to point in the scans because of nonuniform transmission of adjacent fiber-optic bundles. This nonuniformity was removed by observing a tungsten lamp three times per night. Scans of stars and galaxies were divided by the tungsten scan nearest in time. The resultant data therefore yield intensities relative to the tungsten lamp.

At the time division by the tungsten spectrum was performed, the counts were also adjusted for coincidence corrections (effect less than 5%) and reduced to

* *Lick Observatory Bulletin*, No. 714.

a linear wavelength scale (1.25 Å channel^{-1}) using a wavelength calibration provided by scans of helium-argon and neon comparison lamps. Wavelength accuracy is better than 1 Å in all cases, based on residuals from the fit between channel number and wavelength.

The double entrance aperture of the instrument consisted of two identical 2″ × 4″ slits separated by 21″. For stars and most galaxies, the separation was large enough that the signal from the second aperture was negligible. The scan in the second aperture was therefore used as a sky scan. After integration in the first aperture from 4 to 8 minutes, the object was placed in the second aperture. Equal amounts of time were spent in both apertures.

Such a sequence of data was reduced in two ways. In the first, the data were added together. In the second, the series of scans in each channel was reduced separately. Hence one observation yielded three final scans, one from the right channel, one from the left, and one from the data added together. Such a set of three will be termed "one observation."

Standard stars of spectral types G and K were observed each night. Since the standards were too bright to be observed directly, they were dimmed by placing a 2 mag or 5 mag neutral-density filter in front of the slit. The total collection of 60 standard-star spectra provides a continuous monitoring of the instrumental resolution. On any one night, resolution was constant.

Standard observations differed from galaxy observations in two potentially significant ways. In times of good seeing, the star did not fill the full 2″ width of the slit. However, a slit width of 2″ was small enough so that the entire degradation in resolution was caused by the IDS. Thus the effect of underillumination in moments of good seeing should be unimportant. This conclusion is confirmed by the power spectra of stars taken under very different seeing conditions. No systematic differences are present.

Second, exposures for galaxies lasted from 30 to 90 minutes, whereas stellar exposures lasted only 4 to 8 minutes. Long-term drifts in the sweep electronics or flexure in the spectrograph might degrade the resolution in the galaxy scans, but not in the stellar scans. To cause an error greater than 10 percent in the smallest velocity dispersions, drifts of at least 2 Å would be required. Continuous monitoring of the wavelengths of night-sky lines showed that maximum drifts, if any, were less than 0.4 Å. To further check this effect, we computed power spectra of neon scans taken with short and long exposures. Power spectra did not vary as a function of exposure time. Because both of these tests yielded negative results, we believe that differences in exposure time have not introduced a significant source of error.

III. DETERMINATION OF VELOCITY DISPERSIONS

a) Visual Comparison with Broadened Standards

Velocity dispersions were determined in two different ways. In the first, the scans were compared visually with scans of standard stars broadened by various amounts. Four standard scans from each run ranging in spectral type from G8 III to K3 III were transformed to a logarithmic wavelength scale, convolved with Gaussians of various widths, and retransformed to a linear wavelength scale. These standard scans were then superposed on the galaxy spectra, and the best-fitting velocity was determined for each standard spectral type. The identification labels on all galaxy scans were blocked out and the scans were shuffled. Hence the estimates were made without knowing the actual identity of any galaxy.

A single observation of a galaxy provided three scans, each of which was compared with four standard scans. Furthermore both of us made our own independent estimates of the velocities. Thus there were a total of 24 estimates made per observation, providing a high degree of redundancy and facilitating accurate error estimates.

The wavelength range used for matching standards to galaxies covered the region from 4700 to 6000 Å. This region includes Hβ, a strong MgH band, the Mg *b* triplet, the Fraunhofer E line at 5270 Å, Na D, and several other fairly strong lines due mostly to iron-peak elements (see Fig. 1). The matching process was difficult because the galaxy spectra differed systematically from all the standard spectra. In the galaxies, Mg *b*, MgH, and Na D are too strong relative to the remaining lines, probably as a result of a systematically higher metal abundance. This discrepancy could not be resolved by constructing a composite standard spectrum. For this reason we did not construct composite standards but instead we estimated errors due to poor spectral match directly by comparing the results from comparisons with standards of very different spectral types.

In view of our *a priori* ignorance of the true equivalent widths of lines in the galaxy spectra, it would be incorrect to base velocity estimates on the *apparent depths* of the lines. This point has apparently been overlooked in the past (Morton and Chevalier 1973; Richstone and Sargent 1972). Instead of line depths, we based our estimates primarily on certain sensitive blends near Mg *b*, whose appearance depends relatively little on spectral type. With this technique, velocity estimates from G-type standards averaged only three percent lower than estimates from K-type standards. This result is further evidence that use of a composite standard spectrum would not have been significantly more accurate.

Velocities were also estimated from the width of the Na D line, which is independent of spectral type for the standard stars. These averaged 14 percent higher than velocities determined from the region near Mg *b* (Fig. 2). Since the discrepancy is largest in giant elliptical galaxies, which also show the largest enhancement in Na D equivalent width, it may be due in part to a real increase in the intrinsic line width in these galaxies. Matching of the Na D line is also difficult because the continuum in the galaxies is distorted by the presence of TiO absorption not present in the standard stars.

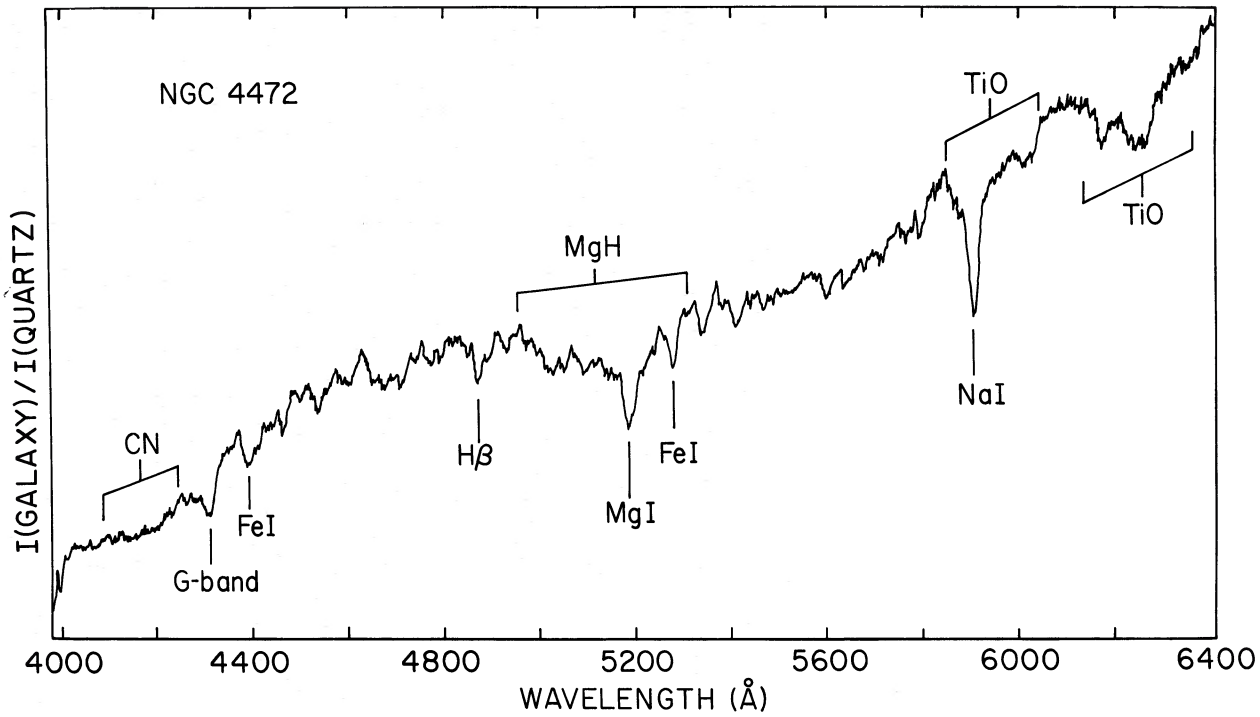

FIG. 1.—Typical scan of giant elliptical galaxy, divided by the tungsten lamp (denoted by "quartz")

In view of the uncertainty in the Na D widths, final averages were computed by assigning twice the weight to the value from the region near Mg *b*. Quadruple weight was given to estimates from the sum of right and left channels combined. Faber and Jackson estimates were weighted equally. Final values of the Mg *b* and Na D velocities, plus the weighted mean visual velocities, are given in Table 1. In this paper, the velocity dispersion v refers to the rms width of the Gaussian distribution function, f, of the line-of-sight radial velocities. Thus $f(x) \propto \exp(-x^2/2v^2)$. A typical match between a galaxy and a standard star in the Mg *b* region is shown in Figure 3.

A comparison of our independent estimates in Figure 4 shows that the systematic difference between the Faber and Jackson velocity scales is less than or equal to 5 percent for both the Mg *b* and Na D values. From comparison of multiple observations, we estimate that the internal rms error of one observation is 10 percent for both the Mg *b* and Na D velocities.

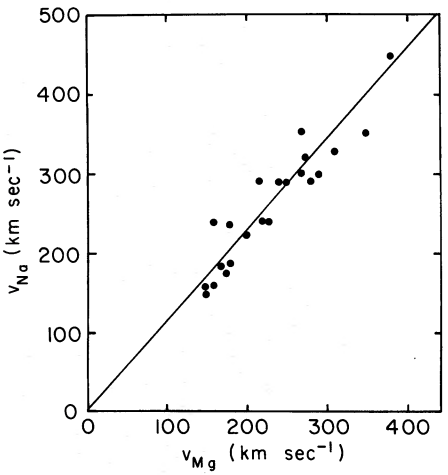

FIG. 2.—Visual velocities from Table 1 determined from the Mg region compared with similar velocities based on the width of Na D. Na D velocities average 14 percent higher (*straight line*).

b) Velocity Dispersions from Power Spectra

Recently Illingworth (Illingworth 1974; Illingworth and Freeman 1974), Simkin (1974), and Peterson (1976), have described the measurement of velocity dispersions for globular clusters and galaxies based on comparisons of power spectra. The method makes use of the convolution theorem for Fourier transforms. Let $g_{gal}(\ln \lambda)$ be the composite spectrum of the galaxy, transformed to a logarithmic wavelength scale, which would be observed if the stars inside the galaxy had no line-of-sight motion relative to one another. Let $f(\Delta \ln \lambda)$ be the velocity distribution function for stars along the line of sight. Then the observed galaxy spectrum is $h_{obs}(\ln \lambda)$ where

$$h_{obs}(\ln \lambda) = \int_{-\infty}^{\infty} f(\ln \lambda - \ln \lambda') g_{gal}(\ln \lambda') d(\ln \lambda') , \quad (1)$$

or

$$h_{obs} = f * g_{gal} . \quad (2)$$

TABLE 1

LINE-OF-SIGHT VELOCITY DISPERSIONS IN GALAXIES

Object	Type	d (Mpc)	M_B (mag)	No. Obs.	Mg** Velocity	Na Velocity	Fourier Velocity(1)*	Fourier Velocity(2)*	Final Visual Velocity	Final Fourier Velocity	Adopted Velocity
M31:	Sb	0.6	-20.3								
Nucleus				3, 1†	180±10‖	183±13‖	170‖	210‖	180‖	190‖	180‖
5" E				1	≤ 150	≤ 150	---	---	≤ 150	---	≤ 150
10" EW				1	≤ 150	≤ 160	185	190	≤ 150	190	≤ 150
15" W				1	175:	175:	---	---	175:	---	175:
20" W				1	160:	≤ 160	---	---	≤ 160:	---	≤ 160:
M32:	E2	0.6	-15.5								
Nucleus				3, 1	≤ 100	≤ 100	100	135	≤ 100	120	≤ 100
5" E				1	≤ 100	≤ 125	---	---	≤ 100	---	≤ 100
10" EW				1	≤ 100	≤ 100	0	90	≤ 100	45	≤ 100
NGC 3115:	S0	8.4	-19.5								
Nucleus				3	270±17‖	353±21‖	283±25‖	320±28‖	300‖	300‖	300:‖‡
5" major axis				2	160±13	160±13	---	---	160	---	160
10" major axis				1	160	240	---	---	190	---	190
15" major axis				1	≤ 180	≤ 180	---	---	≤ 180	---	≤ 180
NGC 3379:	E1	14.8	-20.2								
Nucleus				2	215±24	292±16	235±20	250±0	240	240	240: ‡
10" EW				1	200	225	190:	195:	210	190	210
NGC 3605	E4	16.8	-17.6	2	≤ 125	≤ 125	105±65	135±35	≤ 125	120	≤ 125
NGC 3608	E2	16.8	-19.0	1	220	240	205	240	225	220	225
NGC 3900	S0	33.0	-20.2	1	≤ 150	≤ 150	170	175	≤ 150	170	≤ 150
NGC 4374	E1	23.0	-21.2	2	280±20	290±10	312±67	360±30	285	335	285
NGC 4387	E3	23.0	-18.6	2	≤ 140	≤ 175	178±28	160±12	≤ 150	170	≤ 150
NGC 4406	E3	23.0	-21.3	2	250±20	290±17	258±8	265±5	265	260	265
NGC 4459	S0	23.0	-20.1	2	170±5	184±10	227±38	230±20	175	230	200
NGC 4464	E2	23.0	-18.2	2, 1	≤ 150	≤ 150	85	90	≤ 150	90	≤ 150
NGC 4467	E2	23.0	-16.5	2, 1	≤ 150	≤ 150	70	65	≤ 150	70	≤ 150
NGC 4472	E2	23.0	-22.2								
Nucleus				3	290±6	300±5	292±29	333±24	295	310	295
10" EW				1	270	300	230	265	280	250	280
20" W				2	225±12	240±15	220:	260:	230	240	230
NGC 4478	E2	23.0	-19.4	2	≤ 150	178±20	148±38	160±5	≤ 160	155	≤ 160
NGC 4486	E1	23.0	-21.7	2, 0	310±28	327±29	---§	---§	315	---§	315
NGC 4486B	E0	23.0	-17.5	2	≤ 150	≤ 150	192±5	210±30	≤ 150	200	≤ 150
NGC 4552	E0	23.0	-20.7	2	275±15	320±33	320±25	340±25	290	330	290
NGC 4649	E2	23.0	-21.7	1	360	---	380	405	360	375	360
NGC 4762	S0	23.0	-20.5	1	≤ 150	≤ 150	190	190	≤ 150	190	≤ 150
NGC 4889	E4	140	-22.7	1	380	447	310	455	400	380	400
NGC 5102	S0	6.4	-19.0	1	≤ 150:	≤ 150:	150	140	≤ 150:	145	≤ 150:
NGC 5846	E0	36.0	-21.2	3	240±9	288±8	255±19	290±8	255	270	255
NGC 5846A	E2	36.0	-18.5	1, 0	180	235	---	---	200	---	200
NGC 6166	E	180	-22.7	1	350	350	---	---	350	---	350

* Computed according to methods 1 and 2 (see text).

† When two entries appear, first refers to visual determinations, second to Fourier determination.

‡ Uncertainty larger than average because of large discrepancy between Mg and Na velocities.

‖ May be too large due to effect of nuclear rotation.

§ Fourier method could not be used due to presence of emission lines.

** Determined from region surrounding Mg b.

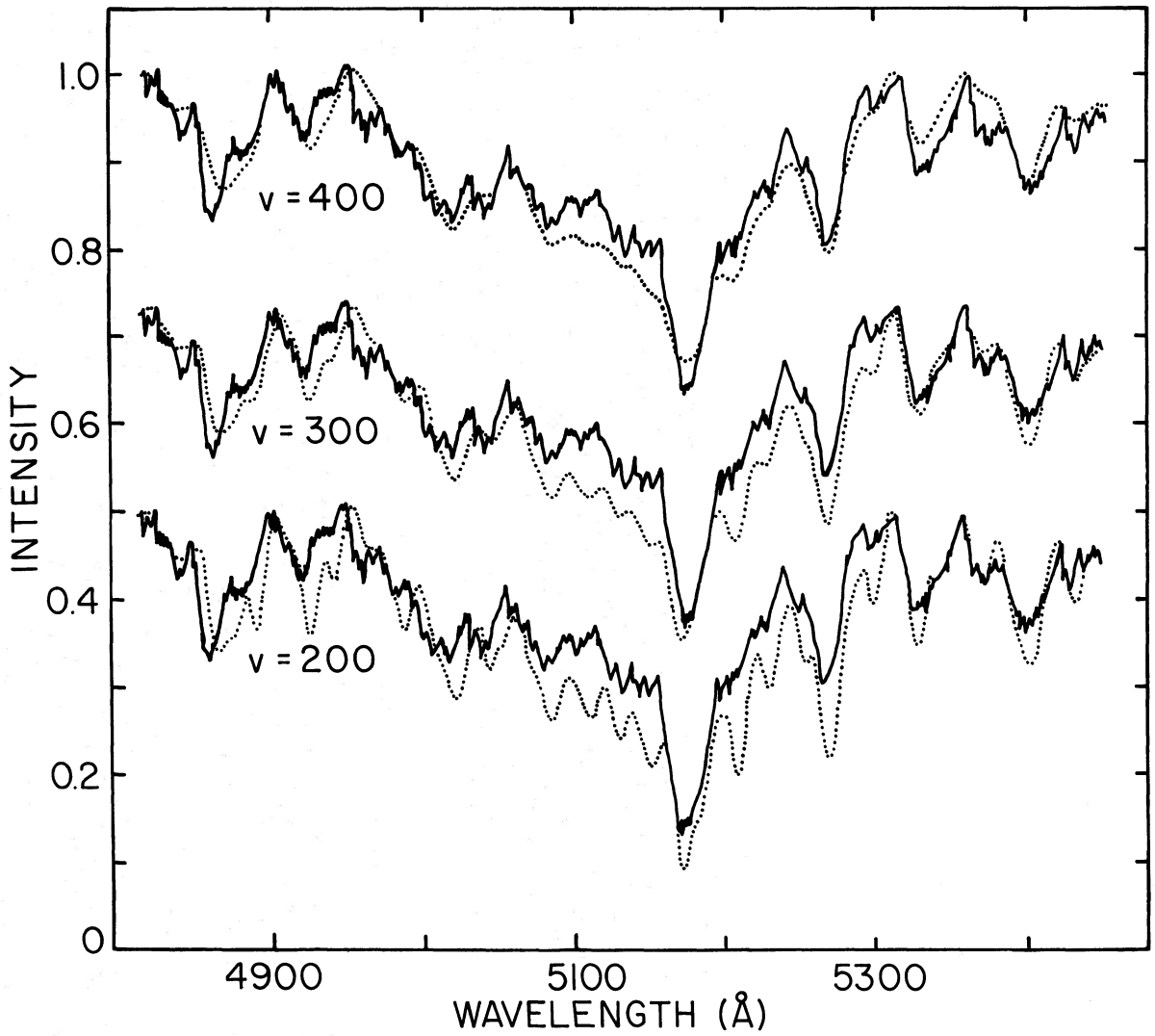

FIG. 3.—NGC 4472 compared with standard star HR 1805 (K3 III), broadened by various line-of-sight velocities (*dotted line*)

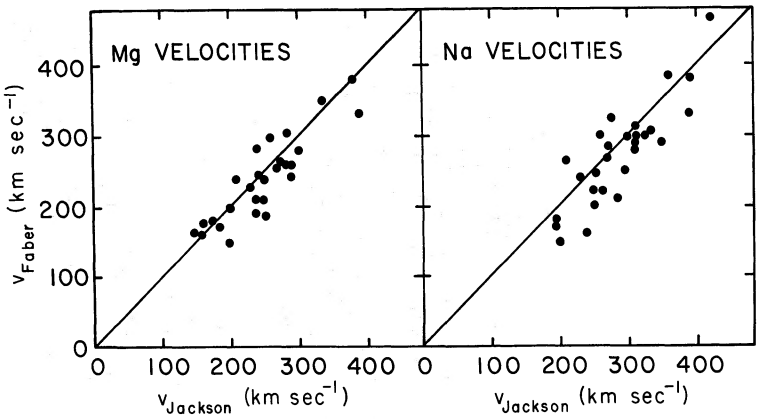

FIG. 4.—Visual velocity estimates of Jackson compared with same estimates by Faber. The one-to-one relation is shown as the straight line. Systematic differences between Jackson and Faber are ≤ 5 percent for both Mg and Na velocities.

Let H_{obs} be the Fourier transform of h_{obs}, etc. According to the convolution theorem,

$$H_{obs} = F \times G_{gal} . \quad (3)$$

Assume that g_{gal} can be satisfactorily represented by the spectrum (or sum of spectra) of standard stars. Then $g_{gal} = g_{std}$. Since we can compute G_{std} and H_{obs} from the observations, F can in principle be determined from equation (3). The value of f is then found by taking the inverse transform of F.

In practice, however, both H_{obs} and G_{std} contain appreciable noise, especially at high frequencies, and the resultant division necessary to obtain F is noisy as well. For this reason, we found it expedient to *assume* that f is a Gaussian function in velocity. We then prepared a set of model transforms, H_{mod}, by multiplying G_{std} by various functions F corresponding to various Gaussian widths for f. The velocity dispersions were then determined by comparing the observed transforms, H_{obs}, with the set of model transforms, H_{mod}. (More precisely, we compared the power spectra $|H_{obs}|^2$ with $|H_{mod}|^2$.) This variant of the Fourier method was also used by Illingworth.[1]

In calculating the power spectra, the fast Fourier transform routine for discrete data was used. The spectra were first transformed to a logarithmic wavelength scale in which one unit equaled 73 km s^{-1}. A 512-point interval from 4798 to 5437 Å in the rest-frame of the object was selected. Unfortunately, this interval, which contains the strongest lines and the best signal-to-noise ratio, also possesses a highly irregular continuum due to the presence of the MgH band (Fig. 1). This feature contributes a great deal of power at all frequencies and must be removed before the power spectra are computed. Using an interactive display terminal, we fitted a smooth curve through the continuum in this region and then divided the spectrum by this smooth function. The result was a flat spectrum with the MgH feature removed. The validity of this procedure is discussed further below.

Before the power spectra were computed, the mean was removed from the data and a 50-channel cosine bell applied to each end. Examples of the input data for a star and galaxy are shown in Figure 5. The resultant power spectra were smoothed with a Gaussian in frequency space with a half-width of five channels, or 1.33×10^{-4} Hz (km s^{-1})$^{-1}$. Power spectra corresponding to the input data in Figure 5 are shown in Figure 6.

To compare $|H_{mod}|^2$ and $|H_{obs}|^2$, it is necessary to use information at high frequencies where noise is important. Hence noise must first be subtracted. We found that the use of mean noise spectra was not sufficiently accurate. A detailed estimate of the noise in each galaxy scan was required. Fortunately such an estimate could be obtained from the power spectrum of the *difference* between the right and left channel in each observation. This power spectrum proved to be a satisfactory estimate of the noise in the summed scan.

A typical smoothed power spectrum of noise is shown in Figure 7. The top scan is the noise spectrum of a galaxy (left channel minus right channel) after division by quartz lamp but before any wavelength reductions were performed on it. This is the raw noise power spectrum of the instrument. It is strongly peaked at low frequencies. This shape can be understood by noting that photons impinging on the first cathode of the intensifier chain are perceived as bursts of photons with finite width on the last phosphor. Hence the noise has nearly the same frequency characteristics as real signals. (The flat, high-frequency component is due to counting statistics in the burst on

[1] Actually, the convolution theorem does not strictly apply to observed galaxy spectra due to truncation of the data. Let $\Pi(\ln \lambda)$ be a unit step function within some specified wavelength interval, and zero elsewhere. Let S be the transform of $\Pi(\ln \lambda)$. Because of the finite range of data collected, h_{obs} is really given by

$$h_{obs} = \Pi \times (f * g_{std}) . \quad (4)$$

Thus
$$H_{obs} = S * (F \times G_{std}) . \quad (5)$$

But
$$H_{mod} = F \times G_{std}' , \quad (6)$$

where
$$g_{std}' = \Pi \times g_{std} , \quad (7)$$

again because of the finite range of data. Hence

$$G_{std}' = S * G_{std} . \quad (8)$$

Thus
$$H_{mod} = F \times (S * G_{std}) . \quad (9)$$

This is not the same as equation (5) because of the different position of S. In words, the effect arises because, in the galaxy, the original infinite spectrum is broadened and then truncated by observation. The model galaxy spectra, on the other hand, are truncated first by observation and then broadened. The order of operations is not commutative.

This problem is of no practical significance as long as S is nearly a δ-function, that is, the interval delimited by Π is sufficiently long. We found that the effect was negligible in the present instance as long as the interval length exceeded 60 Å. This criterion was amply satisfied in our calculations.

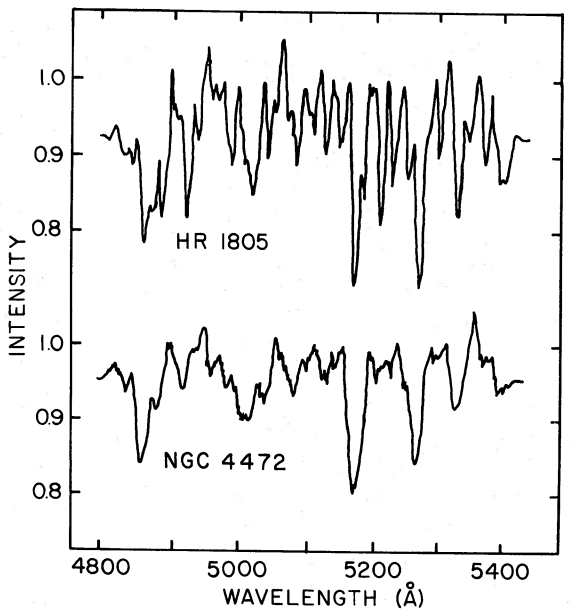

FIG. 5.—Sample input data used to compute power spectra for a standard star (*top*) and a galaxy (*bottom*).

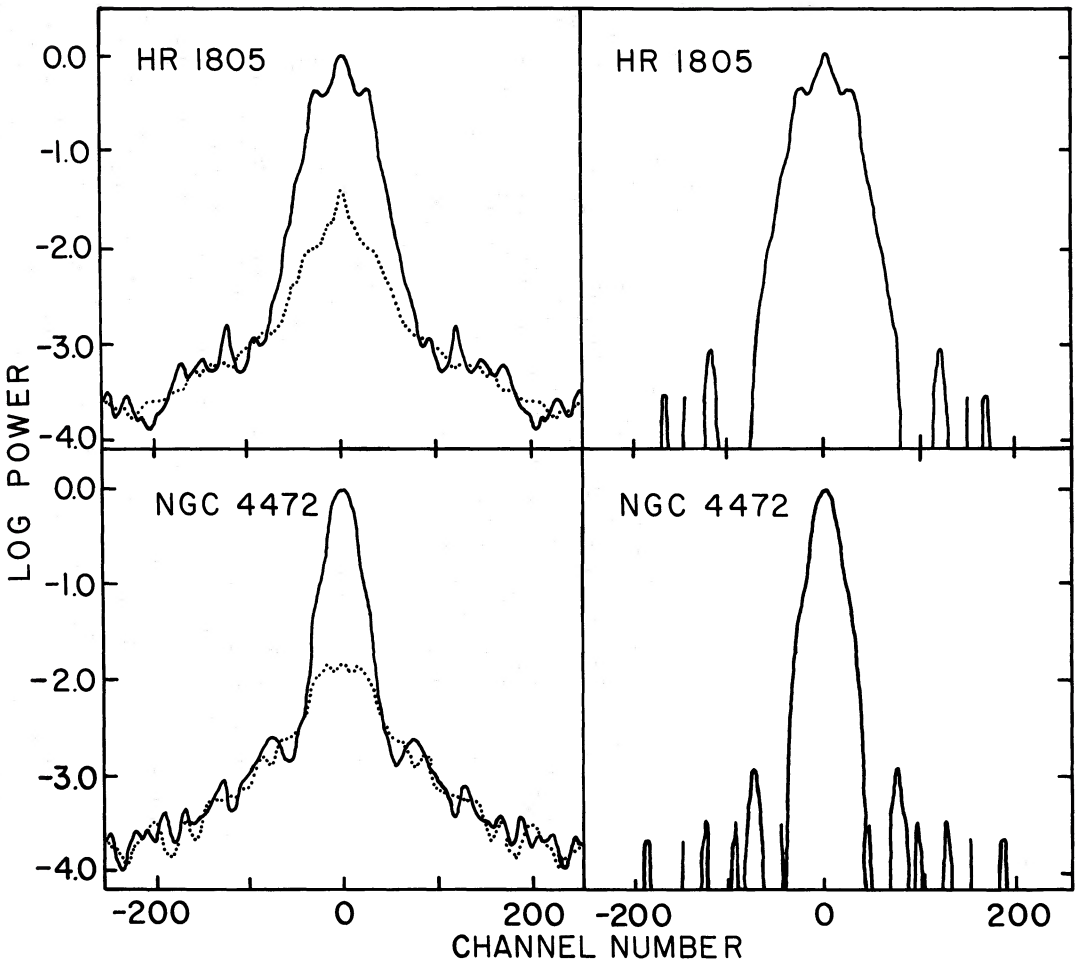

FIG. 6.—Power spectra for a star and galaxy corresponding to the input data in Fig. 5. Noise power spectra are shown by dotted lines. *Left*, raw power spectra including noise. *Right*, power spectra after subtraction of noise.

the last phosphor. This is uncorrelated from channel to channel and hence is white.)

Before the final power spectra were computed, however, the scans were transformed first to a linear and then a logarithmic wavelength scale. Each transformation is an interpolation process and hence smooths the data, reducing the power spectra at high frequencies. This effect can be seen in the second spectrum in Figure 7, which represents the spectrum after both of these interpolations on the data.

To remove the noise, the appropriate noise spectrum was fitted to the corresponding signal spectrum by shifting the logarithmic spectra vertically until the average level agreed in channels 106 to 231. Then the noise was subtracted according to the relation

$$|H_{\rm obs}|^2 = |H_{\rm tot}|^2 - |H_{\rm noise}|^2 , \qquad (10)$$

where $H_{\rm tot}$ corresponds to the observed data consisting of signal plus noise. Power spectra of a star and galaxy after noise removal are shown in Figure 6.

To construct $|H_{\rm mod}|^2$, we removed the noise from standard stellar power spectra and multiplied $|G_{\rm std}|^2$ by $|F|^2$ (see eq. [3]), where F is the transform of velocity-broadening functions of various Gaussian widths.

The remaining step in determining the velocity dispersion entailed a proper comparison between $|H_{\rm obs}|^2$ and $|H_{\rm mod}|^2$. Because of the large amount of data, the procedure had to be fast and convenient. We also desired a method that was impartial, in contrast to the visual comparison in § III*a*, which involved considerable judgment. The procedure adopted is illustrated in Figure 8. The power spectra were plotted on a logarithmic intensity scale, and the area within two decades of the average of the lowest eight channels was measured. A width parameter, $W1$, was defined which represents the width, in frequency channels, of a rectangle having a height of two decades and an area equivalent to the power spectrum. We thought it advisable to check the sensitivity of our results to the adopted definition of the width parameter. Hence, in a variant of the above procedure, the area under the curve corresponding to a level two decades below channel 8 was measured (Fig. 8). The

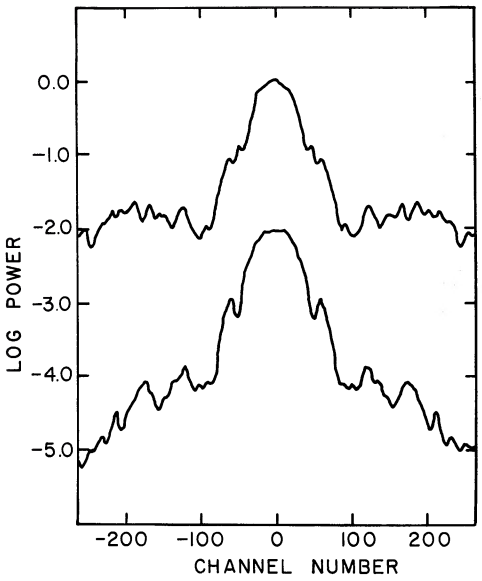

FIG. 7.—Typical power spectra of noise. *Top*, raw power spectrum before reduction to linear and logarithmic wavelength scales. *Bottom*, power spectrum of same data after reduction first to linear and then to logarithmic wavelength scales. Interpolation depresses power spectrum at high frequencies.

corresponding width parameter was called $W2$. We call the two procedures method 1 and method 2, respectively.

The identical parameters $W1$ and $W2$ were measured for the model power spectra, $|H_{\text{mod}}|^2$. Curves were constructed which described the behavior of $W1$ and $W2$ as a function of velocity dispersion. (Fig. 9 shows such curves for the parameter $W2$.) To determine the velocity dispersion of a galaxy, we simply read off the velocity dispersion from the curve using the measured value of $W1$ or $W2$.

This simple procedure was valid because it was found empirically that the W parameters were independent of spectral type and luminosity class (Fig. 10). Hence the constructed W *versus* velocity curves are apparently universal and, in particular, apply to the composite spectra of early-type galaxies.

One additional complication was caused by variable instrumental resolution. The scans fell naturally into three resolution groups, corresponding to different observing sessions. A W-versus-velocity curve was constructed for each group. (These three curves are shown in Fig. 9 for $W2$.) The velocity dispersion of a galaxy was determined by entering $W1$ or $W2$ into the curve for the appropriate instrumental resolution.

To check the correctness of our computer programs as well as to establish the validity of our continuum-straightening procedure (MgH removal), we constructed broadened standard-star spectra by convolving standard stars with Gaussians of known width. Treating these as artificial galaxies, we removed MgH and computed the power spectra, width parameters, and velocity dispersions, using the procedures applied to the normal galaxies. The velocity dispersions obtained in this way, using either method 1 or method 2, agreed virtually perfectly with the actual values. This good agreement indicates that our measurement procedures, and, in particular, our method for removing MgH, introduce no systematic errors.

The results of the two Fourier methods are listed in Table 1. The two velocity systems agree within 15 percent. Inspection of the errors indicates that the rms error is 20 percent for method 1 and 10 percent for method 2 for one good observation. However, this error estimate is unrealistically low. We found that the Fourier method is actually very sensitive to noise. In several cases, v could not be computed from the power spectrum because it was too noisy to be useful, even though the data yielded acceptably accurate velocity dispersions using the visual comparison method. These noisy cases were not included in the table.

The mean Fourier and mean visual velocities are compared in Figure 11. The systematic difference between the two scales is 5 percent or less. This result

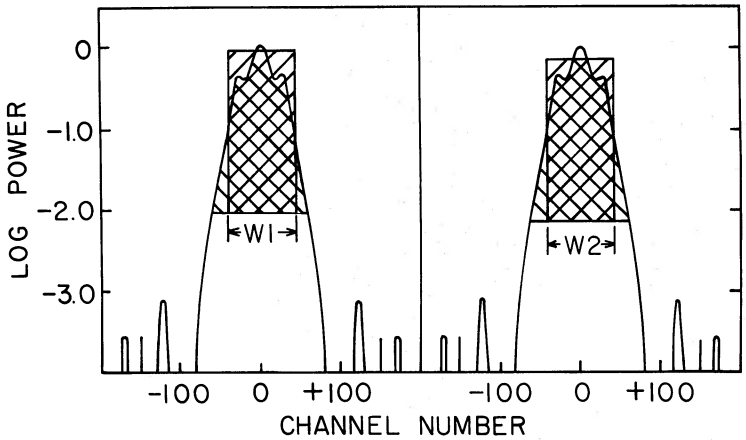

FIG. 8.—Definition of width parameters $W1$ and $W2$. Area under rectangle equals hatched area under power-spectrum profile. Height of rectangles is 2.0 in log (power). *Left*, parameter $W1$. Upper edge of rectangle corresponds to logarithmic average of channels 0 through 8. *Right*, parameter $W2$. Upper edge of rectangle corresponds to level in channel 8.

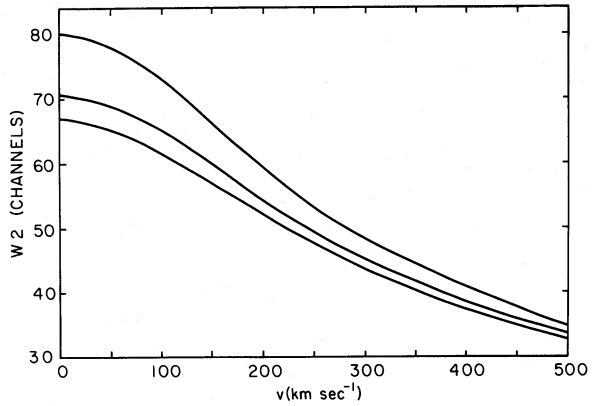

FIG. 9.—Width parameter $W2$ as a function of line-of-sight velocity dispersion as determined from model power spectra. The three curves correspond to three different values of the instrumental resolution. Curves for $W1$ are similar.

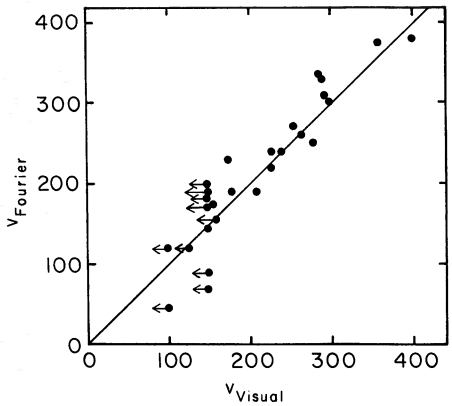

FIG. 11.—Visual velocities versus Fourier velocities from Table 1. The straight line is the one-to-one relation. Arrows denote upper limits.

suggests that the systematic errors in both visual and Fourier velocities are small. However, we recall that the Na D velocities differed from the Mg *b* velocities by 15 percent, and that the two Fourier methods disagreed by a similar amount. It seems safer to admit that residual scale errors on the order of 10–15 percent might still be present.

As our final values, we have adopted the visual means since the visual method was less sensitive to noise and was used independently by each of us with consistent results. These adopted values are given in Table 1.

In pursuing the Fourier approach we hoped for an increase in accuracy of the kind found by Illingworth. To our disappointment, the Fourier method seemed overly sensitive to noise. This fact is due to the much smaller signal-to-noise ratio inherent in the galaxy scans as a result of the shallowness of the absorption lines. The lines in Illingworth's globular clusters, by contrast, are quite deep because velocity dispersions in globular clusters are small.

However, the Fourier method was totally impartial and was also insensitive to spectral type (Fig. 10).[2] This insensitivity to spectral match is in accord with our conclusion in § III*a* that velocity dispersions can be determined without recourse to composite spectra. This result disagrees with de Vaucouleurs's (1974) statement that the compositeness of galaxy spectra leads to a "spurious" line broadening.

In the present study, we feel that the added effort necessary for the Fourier technique was worthwhile because the reasonable agreement between the visual and Fourier velocities suggests that both scales are free of large errors. The general validity of our visual scale now having been established, however, future velocity-dispersion measurements will be made using only the visual method.

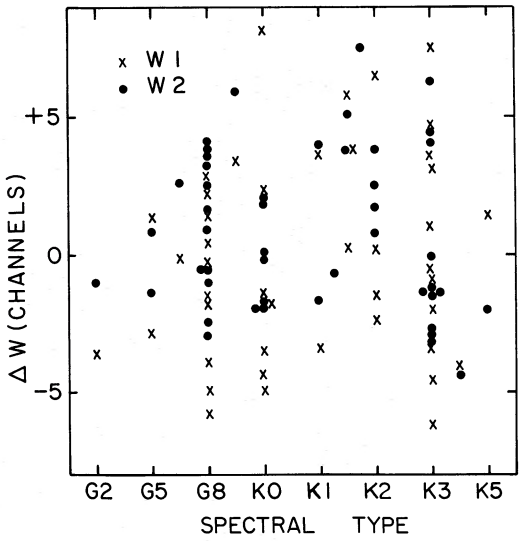

FIG. 10.—Width parameters $W1$ and $W2$ versus spectral type. Mean values of $W1$ and $W2$ were calculated for each observing run. $\Delta W = W - \overline{W}$. The residuals ΔW show no significant trend with spectral type.

IV. COMPARISON WITH PREVIOUS OBSERVATIONS

Table 2 compares our velocity dispersions with previously measured values. Figure 12 shows that our velocities are significantly smaller than Minkowski's (1962), an effect confirmed by the recent work of several other individuals (Morton and Thuan 1973; Richstone and Sargent 1972; de Vaucouleurs 1974).

Even after one sets aside the Minkowski values, the remaining data in Table 2 are cause for dismay. Agreement among the various values is worse than expected from the quoted errors. A few entries deserve special comment. Morton and Thuan (1973) have

[2] Insensitivity to spectral type is due to the fact that, if a large number of absorption lines are present in the interval, the resultant power spectrum is the spectrum of an individual line profile. In our case, the line profile is determined by the instrument, and hence is the same for all standard stars. It is curious, but easily proven, that matching in the power-spectrum domain is insensitive to spectral type, whereas similar matching (for example, by least-squares minimization) between galaxy and standard star in the original spectral domain is sensitive to spectral match.

TABLE 2

COMPARISON WITH OTHER PUBLISHED VALUES

OBJECT	v ADOPTED (km s^{-1})	OTHER SOURCES* [1]	[2]	[3]	[4]
M31	180†	225	...	150	120
NGC 3115, nuc	300:†	...	...	230*	215
NGC 3115, 10″	170	205	...	...	160
NGC 3379	240:	...	187	125	...
NGC 4406	265	415	...	...	...
NGC 4472	295	365	...	...	...
NGC 4486	315	490	...	...	...
NGC 4486B	≤150	370	...	160:	...
NGC 4762	≤150	195	...	...	...

* [1] Minkowski (1962); [2] Burbidge *et al.* (1961); [3] de Vaucouleurs (1974); [4] Morton and Chevalier (1973), Morton and Thuan (1973).

† May be affected by nuclear rotation.

measured the nuclear velocity dispersion in M31 and obtained 120 km s^{-1}. However, inspection of their published scans indicates that a velocity of at least 150 km s^{-1} is a much better fit to their data. The best fit might be even larger, but they do not show model spectra for larger velocities. Given that our value, corresponding to a 2″ × 4″ slit, might contain some contribution from nuclear rotation (Walker 1975), our value is not necessarily in disagreement with either the Morton-Thuan result or the value of 150 km s^{-1} given by de Vaucouleurs (1974).

NGC 3115, however, is more distressing. We obtain 300 km s^{-1}, whereas Morton and Chevalier (1973) and de Vaucouleurs (1974) measure much smaller values of 215 and 230 km s^{-1}. Furthermore our value for NGC 3379 of 240 km s^{-1} is grossly at variance with de Vaucouleurs's measurement of 125 km s^{-1}. By sheer bad luck, our values for NGC 3115 and 3379 are among our most uncertain, because both of these objects give rather different results depending on whether the Mg b area or the Na D line is used. Even so, the disagreement with other published values is discouragingly large. (In Figs. 13, 14, and 15 we present fits between galaxy and standard stars for M31, NGC 3115, and NGC 3379.)

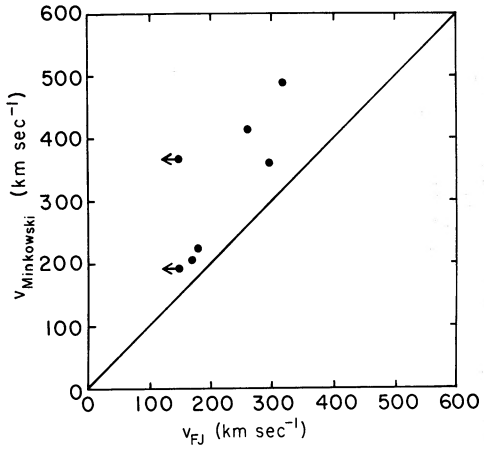

FIG. 12.—Comparison between Minkowski's (1962) velocity dispersions and those measured in this paper.

What is the explanation for these discrepancies? We have at least two separate observations of each object, and the broadenings in the different scans of the same galaxy are identical within the errors of measurement. The Fourier values also support our visual estimates. Finally, in the next section we show that for normal ellipticals, velocity dispersion is closely correlated with absolute magnitude. De Vaucouleurs's low value for NGC 3379, for example, would be inconsistent with the smooth trend displayed by the other galaxies.

For all these reasons we prefer our measurements to those previously published, but in view of the persistent disagreement among the various workers in this field, we are reluctant to claim we have spoken the last word.

V. RESULTS AND DISCUSSION

Dr. Ivan King has kindly communicated to us in advance of publication his measurements of core radii and central surface brightness for several galaxies in our sample. Using his method (King and Minkowski 1972), we have calculated nuclear values of the mass-to-light ratio (M/L_B) for these galaxies. This method includes an approximate correction for rotational motions.[3]

For galaxies outside the Local Group, distances

[3] Because the velocity dispersion in the halo of an elliptical galaxy is smaller than that in the core, the projected velocity dispersion as measured is smaller than the true core velocity dispersion, which is required by King's method. Using King's model for the Coma cluster (King 1972), which is also a good fit to the typical elliptical NGC 3379, we calculate that the projected velocity dispersion is only 2 percent smaller than the core value. King's model assumes that the velocity dispersion is isotropic throughout. In models which incorporate eccentric orbits, the tangential component of the dispersion decreases rapidly away from the core, but the radial component is much more constant (e.g., Gott 1974). It is this radial component, of course, which contributes to the line-of-sight velocity dispersion measured through the nucleus. Hence it seems safe to assume that the core velocity dispersion is actually quite close to the projected, measured value.

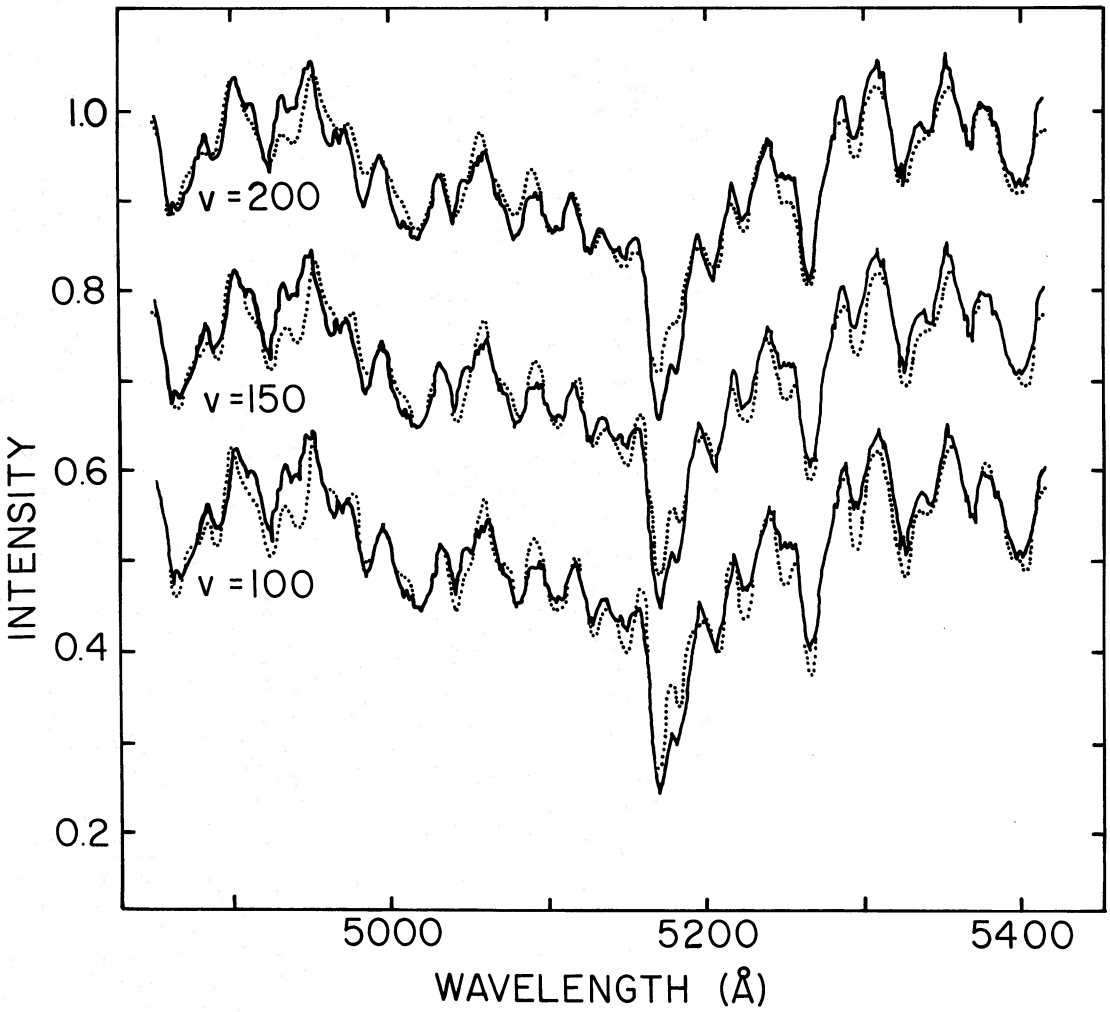

FIG. 13.—The nucleus of M31 compared with broadened spectra of standard star HR 2600 (K2 III) (*dotted line*). Adopted mean visual velocity is 180 km s^{-1}. (Sum of two observations.)

corresponding to a Hubble constant H of 50 km s^{-1} Mpc^{-1} were assumed. For galaxies in groups and clusters, a mean group or cluster velocity was used. To obtain the absolute magnitudes, a correction for galactic absorption of the form $A_B = 0.20 \csc |b|$ was applied to the observed apparent galaxy magnitudes $B(0)$, taken from the *Reference Catalogue of Bright Galaxies* (de Vaucouleurs and de Vaucouleurs 1964).

Results are shown in Table 3. The mean M/L_B for giant ellipticals with $M_B < -20$ is $7(H/50)$ in solar units, considerably lower than the mean value of roughly $15(H/50)$ quoted by King and Minkowski for a similar selection of objects. Most of the change is due to the lower velocity dispersions presented here, but our correction for galactic absorption has also introduced an additional decrease of approximately 20 percent. Lower values of M/L_B have already been suggested by the work of Morton and co-workers (Morton and Chevalier 1972, 1973; Morton and Thuan 1973) and by de Vaucouleurs (1974).

These lower values of M/L_B are evidence against the strongly dwarf-enriched stellar population inferred by Spinrad and Taylor (1971) from photometric scans of the nucleus of M31. Our results agree with the conclusions of subsequent investigators (Faber 1973; Baldwin, Frogel, and Persson 1973; Whitford 1974; O'Connell 1974) which have indicated that the light from M31 and giant ellipticals in fact contains very little contribution from M dwarfs.

These smaller values of M/L also compare favorably with M/L's for early-type spirals. Nordsieck (1973) has shown that, for spiral and Irr I galaxies, M/L is related to color and hence to stellar population. If his data are converted to a Hubble constant of 50 km s^{-1} Mpc^{-1}, M/L_B for the reddest, earliest-type spirals is roughly 5.5. This value agrees nicely with the average value for massive ellipticals of 7 quoted above. The techniques for measuring M/L are of course very different for ellipticals and spirals. If we assume that there is no systematic difference between the two

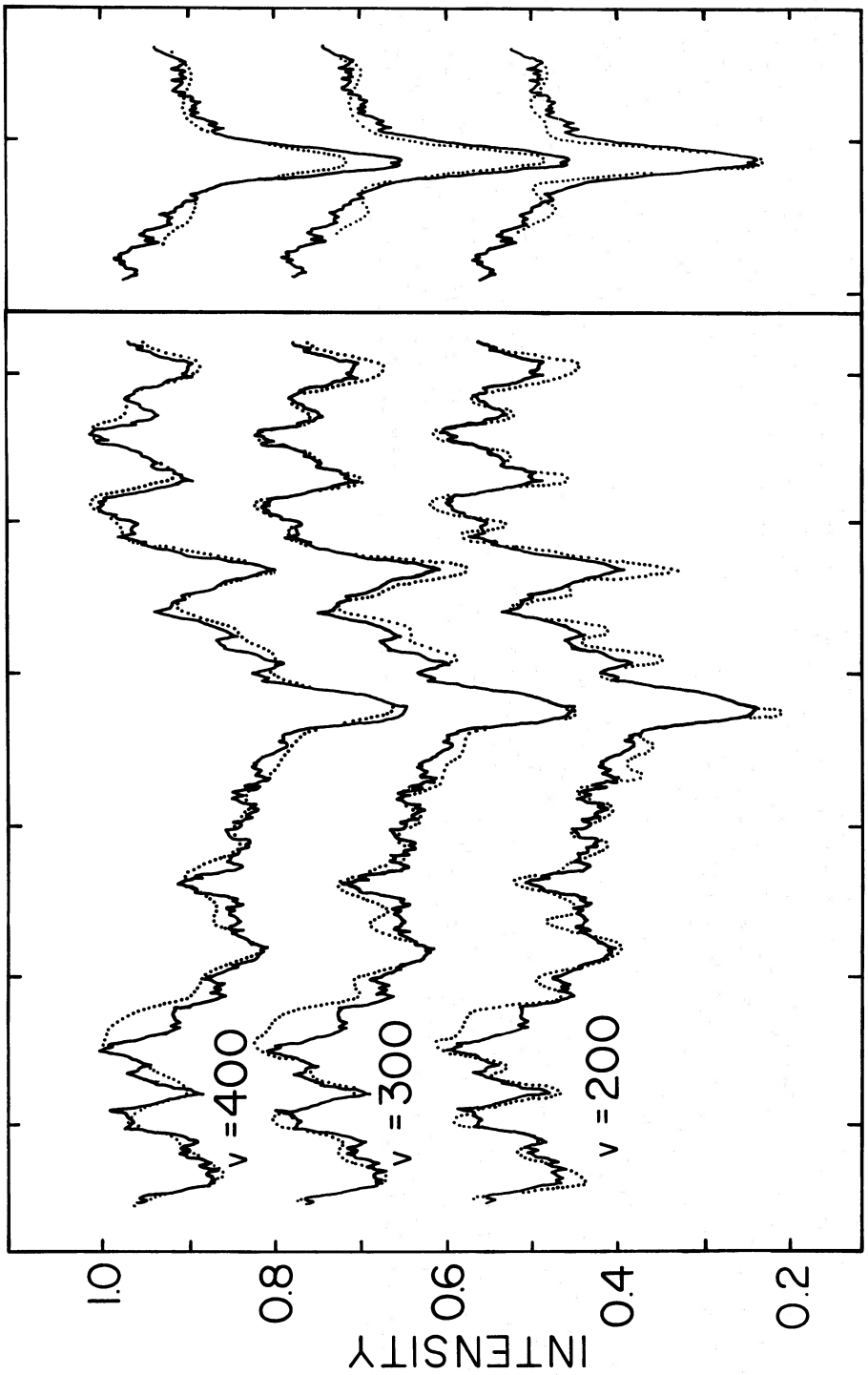

FIG. 14.—The nucleus of NGC 3115 compared with broadened spectra of standard star HR 3905 (K2 III) (*dotted line*). *Left*, Mg *b* region. *Right*, Na D region. Adopted mean Mg velocity is 270 km s^{-1}. For this object the discrepancy between Mg and Na is larger than average. (Sum of two observations.)

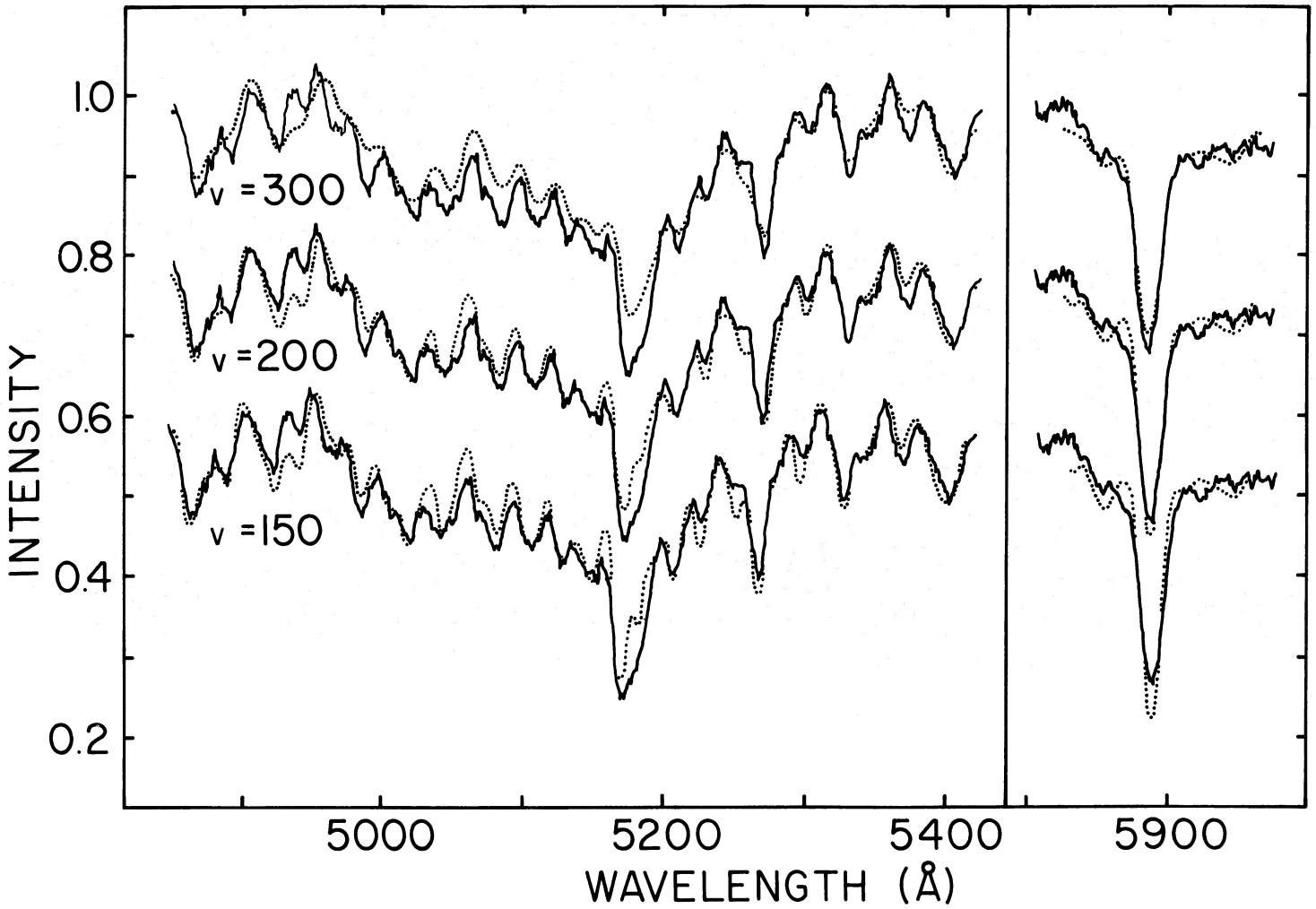

FIG. 15.—NGC 3379 compared with broadened spectra of standard stars (*dotted line*). *Left*, Mg *b* region. Standard star is HR 3905 (K2 III). *Right*, Na D region. Standard star is HR 2600 (K2 III). Adopted mean Mg velocity is 215 km s^{-1}. Adopted mean Na velocity is 292 km s^{-1}. For this object the discrepancy between Mg and Na is larger than average. (Sum of two observations.)

TABLE 3

MASS-TO-LIGHT RATIOS

Object	v (km s^{-1})	M_B (mag)	M/L_B* (solar units)
NGC 3379.....	240	−20.2	5.4
NGC 4374.....	285	−21.2	5.3
NGC 4406.....	265	−21.3	6.8
NGC 4459.....	200	−20.1	4.4
NGC 4472.....	295	−22.2	5.0
NGC 4486.....	315	−21.7	10.2
NGC 4486B.....	≤150	−17.5	≤3.8
NGC 4552.....	290	−20.7	5.7
NGC 4649.....	360	−21.7	9.3
NGC 4889.....	400	−22.7	11.5
NGC 5846.....	255	−21.2	8.3

* Corrected for galactic absorption using $A_B = 0.20\ |\csc b|$ and assuming $H = 50$ km s^{-1} Mpc^{-1}.

methods, there is apparently no evidence for a large discontinuity in M/L_B between Sa's and E's. This conclusion agrees with the fact that the color change (and hence presumably the change in stellar population) between Sa's and E's is also small.

If these nuclear values of M/L_B are assumed to apply to entire galaxies, however, the problem of the "missing mass" in clusters of galaxies has worsened. For example, correcting M/L_B found by Rood *et al.* (1972) for the Coma cluster to $H = 50$, we obtain $M/L_B \approx 170$. If M/L_B for the average elliptical is 7, the mass discrepancy is a factor of 25 instead of only 12. Likewise, our new value is marginally inconsistent with Page's (1965) data on double galaxies, which yielded $M/L_B = 45 \pm 18$ ($H = 50$). The arguments which interpret these data as evidence for massive halos of galaxies are well known (e.g., Ostriker, Peebles, and Yahil 1974) and will not be repeated here.

Perhaps the most interesting result to emerge from the present study is an indication that both velocity dispersion and M/L_B are correlated with absolute magnitude for normal elliptical galaxies. The relation between $\log v$ and M_B is shown in Figure 16. In view of the scatter, it seems adequate to represent the data by the relation $L_B \propto v^4$. Such a correlation between v and M_B was initially suggested by Minkowski (1962), based on fragmentary data. (More recently, Morton and Chevalier [1973] have argued against such a correlation between v and luminosity, but their conclusion rests largely on an erroneous assumed distance for NGC 4473 based on its redshift. NGC 4473 is probably a high-redshift member of the Virgo cluster [Humason, Mayall, and Sandage 1956; de Vaucouleurs 1961].)

None of the elliptical galaxies in the present sample is highly flattened. Since extreme flattening would imply large rotational motions, we might expect smaller random motions in flattened ellipticals. It would be interesting to study a sample of highly flattened ellipticals to see if their velocity dispersions are systematically smaller than those measured in the present sample.

King has measured preliminary core radii and central surface brightnesses for a large sample of luminous ellipticals with $M_B < -20$. Our study of his data indicates that both of these quantities are also broadly correlated with absolute magnitude. Expressing these relationships in terms of power laws and combining these results with the relation $L_B \propto v^4$, we would predict that $M/L_B \propto L_B^{1/2}$. This result is compared with the observed values of M/L_B in Figure 17. Except possibly for NGC 4472, the prediction is reasonably consistent with the observations.

The source of scatter in these apparent correlations between velocity dispersion in luminosity, surface brightness, and core radius is a matter of some interest. Some portion is of course due to observational error, but our impression is that some fraction is intrinsic to the objects. More attention will be paid to the sources of scatter in a forthcoming paper in which the data on core radius, surface brightness, and luminosity will be discussed in greater detail.

The present data are valuable because they form a homogeneous set of observations which have been

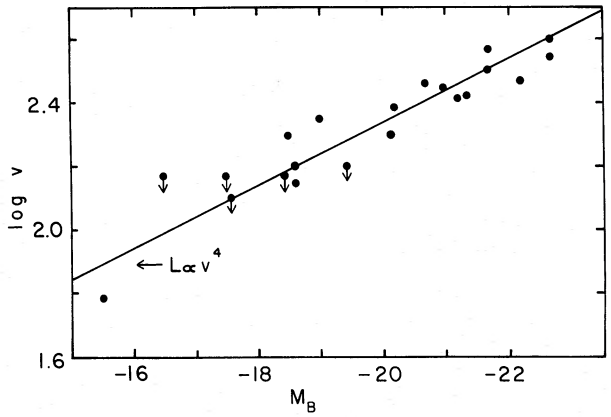

FIG. 16.—Line-of-sight velocity dispersions versus absolute magnitude from Table 1. The point with smallest velocity corresponds to M32, for which the velocity dispersion (60 km s^{-1}) was taken from Richstone and Sargent (1972).

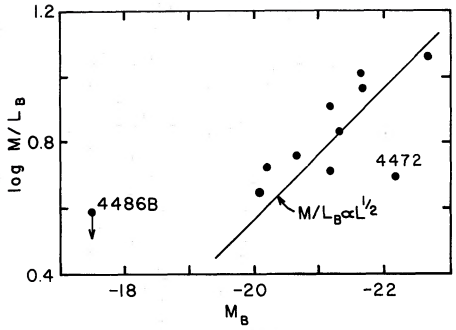

FIG. 17.—Mass-to-light ratio in solar units versus absolute magnitude from Table 3. The predicted relation based on King's data and on the power-law $L \propto v^4$ is shown as the straight line.

treated in a consistent fashion. For this reason, trends of the sort shown in Figures 16 and 17 are not masked by systematic differences between various investigators. At the risk of introducing such errors into our discussion, we mention that Hodge (1971) obtains an M/L_B near 1 for the Sculptor dwarf spheroidal system based on its tidal radius and a total mass for the Milky Way of $2 \times 10^{11} M_\odot$. Although extremely uncertain, this value is in general agreement with the increasing trend in M/L_B defined by the more luminous galaxies. Others (most recently Einasto [1972] and Einasto and Kaasik [1974]) have suggested that there is a correlation between M/L and mass for spheroidal galaxies. Our new data show the same behavior, but the effect is considerably smaller because M/L for the most massive galaxies has been reduced.

We do not place any physical significance on these power-law-relationships, which we regard merely as convenient representations of the data. In particular, we know that at least the power-law relation for surface brightness breaks down at lower luminosities, because the surface brightness reaches a maximum near $M_B \approx 19$–20 (Oemler 1973) and then declines again at smaller luminosities. This fact implies that the exact power-law relation between M/L_B and L_B will also fail to hold for fainter luminosities. (However, the power law in v versus L_B appears to be valid over a large range of absolute magnitude [Fig. 16].)

It is well known that the colors and line-strengths of normal elliptical galaxies are closely correlated with absolute magnitude (Faber 1973; Sandage 1972). The present results indicate that the dynamical properties and mass-to-light ratios are likewise broadly correlated. Indeed, the available evidence supports the conclusion that, in most respects, the elliptical galaxies are close to being a one-parameter family with total mass as the most important independent variable.

We offer the following tentative hypothesis to explain the observed dependence of M/L_B on luminosity in Figure 17. Suppose that the initial mass function for star formation is a constant in luminous elliptical galaxies independent of galaxy mass. The evidence from spectra and colors indicates that the giant E's are more metal-rich than the fainter ellipticals. An increase in metals decreases the luminosity of main-sequence stars and has an even larger effect in depressing the luminosity of the giant branch (compare, for example, the old disk giant branch with a typical globular cluster). Hence, of two essentially similar stellar populations which differ only in metal content, the more metal-rich will be fainter in blue light and have larger M/L_B. Detailed calculations of the integrated properties of old stellar populations as a function of abundance are planned to test whether the exact behavior of M/L_B can be explained in this way.

Lastly, the present data contain weak evidence for a decline in velocity dispersions away from the nuclei. This effect is most dramatic in NGC 3115 and is confirmed by the scans of Morton and Chevalier (1973). In this object, which is a borderline S0 galaxy, one sees principally the disk component on the major axis away from the nucleus. Thus it is not surprising that a lower velocity dispersion is measured in this cooler, disk component.

VI. SUMMARY

Velocity dispersions for 25 galaxies have been measured using conventional and Fourier techniques. The resultant velocity system is probably accurate to 10–15 percent. Internal rms errors are of the order of 10 percent.

Using King's values of core radii and central surface brightnesses, we compute nuclear values of M/L_B. For giant ellipticals with $M_B < -20$, we obtain an average value of only $7(H/50)$. This value agrees well with the values of M/L_B for early-type spirals. In particular, it implies that there is no large discontinuity in M/L between early-type spirals and ellipticals, a result consistent with the small observed color changes between Sa's and ellipticals.

Velocity dispersion increases with absolute magnitude for normal E's of moderate ellipticity. The data are consistent with the relation $L_B \propto v^4$. The data also suggest a positive correlation between M/L_B and L_B, and this conclusion is supported by King's data on core radii and surface brightnesses, to be discussed fully in a separate paper. The observed increase in M/L is consistent with a probable increase in metal abundance with luminosity. Perhaps the entire effect is due to this mechanism. The close correlation between luminosity and dynamical properties among normal ellipticals is further evidence that the elliptical sequence is very nearly a one-parameter family. These results clearly are of importance to any theory of elliptical formation.

Discussion of the absorption-line-strengths plus the behavior of velocity dispersions and line-strengths away from the nucleus in E and S0 galaxies will form the subject of future papers in this series.

We would like to thank Drs. L. Robinson and J. Wampler for their help in using the image-dissector scanner. We are particularly grateful to Dr. Ivan King for communicating his unpublished data and for many fruitful discussions.

REFERENCES

Baldwin, J. R., Frogel, J. A., and Persson, S. E. 1973, *Ap. J.*, **184**, 427.
de Vaucouleurs, G. 1961, *Ap. J. Suppl.*, **6**, 213.
———. 1974, in *IAU Symposium No. 58, Formation and Dynamics of Galaxies*, ed. J. R. Shakeshaft (Dordrecht: Reidel), p. 1.
de Vaucouleurs, G., and de Vaucouleurs, A. 1964, *Reference Catalogue of Bright Galaxies* (Austin: University of Texas Press).
Einasto, J. 1972, *Tartu Astr. Obs. Preprint* No. 40.
Einasto, J., and Kaasik, A. 1974, cited by de Vaucouleurs 1974, p. 22.
Faber, S. M. 1973, *Ap. J.*, **179**, 731.
Fish, R. A. 1964, *Ap. J.*, **139**, 284.
Gott, J. R., III. 1974, preprint.
Hodge, P. W. 1971, *Ann. Rev. Astr. and Ap.*, **9**, 35.
Humason, M. L., Mayall, N. U., and Sandage, A. R. 1956, *A.J.*, **61**, 97.
Illingworth, G. 1974, unpublished Ph.D. thesis, Australian National University.
Illingworth, G., and Freeman, K. C. 1974, *Ap. J. (Letters)*, **188**, L83.
King, I. R. 1972, *Ap. J. (Letters)*, **179**, L123.
King, I. R., and Minkowski, R. 1972, in *IAU Symposium No. 44, External Galaxies and Quasi-stellar Objects*, ed. D. S. Evans (Dordrecht: Reidel), p. 87.
Minkowski, R. 1962, in *IAU Symposium No. 15, Problems of Extra-galactic Research*, ed. G. McVittie (New York: Macmillan), p. 112.
Morton, D. C., and Chevalier, R. 1972, *Ap. J.*, **174**, 486.
———. 1973, *ibid.*, **179**, 55.
Morton, D. C., and Thuan, T. X. 1973, *Ap. J.*, **180**, 705.
Nordsieck, K. H. 1973, *Ap. J.*, **184**, 735.
O'Connell, R. 1974, *Ap. J. (Letters)*, **193**, L49.
Oemler, A., Jr. 1973, *Ap. J.*, **180**, 11.
Ostriker, J. P., Peebles, P. J. E., and Yahil, A. 1974, *Ap. J. (Letters)*, **193**, L1.
Page, T. L. 1965, *Smithsonian Institution Ap. Obs.*, Spec. Rep. No. 195.
Peterson, C. 1976, to be published.
Richstone, D., and Sargent, W. L. W. 1972, *Ap. J.*, **176**, 91.
Robinson, L., and Wampler, E. J. 1972, *Pub. A.S.P.*, **84**, 161.
Rood, H. J., Page, T. L., Kintner, E. C., and King, I. R. 1972, *Ap. J.*, **175**, 627.
Sandage, A. R. 1972, *Ap. J.*, **176**, 21.
Simkin, S. 1974, *Astr. and Ap.*, **31**, 129.
Spinrad, H., and Taylor, B. 1970, *Ap. J. Suppl.*, **22**, 445.
Walker, M. 1974, *Pub. A.S.P.*, **86**, 861.
Whitford, A. E. 1974, in *IAU Symposium No. 58, Formation and Dynamics of Galaxies*, ed. J. R. Shakeshaft (Dordrecht: Reidel), p. 169.

S. M. FABER and ROBERT E. JACKSON: Lick Observatory, University of California, Santa Cruz, CA 95064